La mer 37 : 45–57, 1999
Société franco-japonaise d'océanographie, Tokyo

Dependence on the vertical eddy diffusivity for the oceanic circulation in the Okhotsk Sea

Fukuji YAMADA* and Yoshihiko SEKINE*

Abstract : Oceanic circulation in the Okhotsk Sea is examined numerically with special reference to its dependence on the intensity of vertical eddy diffusivity. Firstly, three models with different coefficient of vertical eddy diffusivity are driven by the observational annual mean wind stress with adiabatic surface condition. Secondly, three models are driven by the observed wind stress and heat flux through the sea surface. Thirdly, two models are driven by the wind stress, the heat flux and salinity flux, which are recovering the observed temperature and salinity at the sea surface. It is commonly resulted that cyclonic circulation is formed east of Sakhalin and relatively strong flow is generated along western coast of Sakhalin and Hokkaido. The volume transport function has a tendency to flow along isobath of bottom topography and velocity field has a barotropic structure with vertical coherency. These results imply that wind driven circulation is dominant in the Okhotsk Sea in comparison with thermohaline circulation. However, temperature and salinity distributions in the Okhotsk Sea are influenced by intensity of vertical eddy diffusivity. It is thus concluded that the oceanic circulation in the Okhotsk Sea is almost independent from the intensity of vertical eddy diffusivity.

Keywords *: Okhotsk Sea, thermohaline circulation, vertical eddy diffusivity*

1. Introduction

The Okhotsk Sea is a marginal sea of the North Pacific and is surrounded by Kamchatka Peninsula, Siberia, Sakhalin Island, Hokkaido and Kuril Islands. There is a broad continental shelf along Kamchatka Peninsula and Siberian coasts, while a relatively deep basin exists in a southern portion. A characteristic features in the Okhotsk Sea are an in-and outflow of the Oyashio through some straits in the Kuril Islands and the Soya Warm Current, which flows through the Soya Strait and flows out though straits in the southern Kuril Islands.

Some observational studies on the oceanic circulation in the Okhotsk Sea have been carried out (KAJIURA, 1949; MOROSHKIN, 1964; KITANI and SHIMAZAKI, 1971; KITANI, 1973; KURASHINA, 1986; WAKATSUCHI and MARTIN, 1991). SEKINE (1990) examined the wind-driven circulation in the Okhotsk Sea by use of a barotropic numerical model and showed that the wind-driven circulation dominates in winter, while the circulation is mainly driven by in-and outflow in summer. However, because of homogeneous model assumption, the baroclinic structure was not considered in his study. As there exists stratification in the Okhotsk Sea, to examine the effect of density stratification is needed for the general circulation in the Okhotsk Sea. In relation to this, it is well-known that numerical oceanic circulation is much influenced by the intensity of vertical eddy diffusivity (e.g., BRYAN, 1987; ZHANG *et al.*, 1992) : the wind driven circulation dominates, if small vertical eddy diffusivity is assumed, while the thermohaline circulation dominates in cases with large vertical diffusivity.

In the present study, we numerically examine wind and thermohaline driven circulations in the Okhotsk Sea with special reference to their dependence on the intensity of vertical eddy diffusivity. In the following, detailed descriptions of the used model and data will be made in sections 2 and 3, respectively. The result of the numerical experiment will be

* Institute of Oceanography,
Faculty of Bioresources, Mie University,
1515 Kamihama-chou, Tsu, Mie 514-8507
Japan

Table 1. List of symbols

t	time
u, v	horizontal component of the velocity in the x-and y-directions
f	Coriolis parameter ($f=f_0+\beta_x x+\beta_y y, f_0=1.01\times10^{-4}$ sec^{-1})
β_x, β_y	linear change rate of the Coriolis parameter ($\beta_x=\beta_y=9.22\times10^{-14}$cm^{-1} s^{-1})
ρ_0	density averaged over the whole ocean (1.027 g cm^{-3})
P	pressure
A_H	horizontal eddy viscosity coefficient (1.0×10^7 cm^2 sec^{-1})
A_V	vertical eddy viscosity coefficient (5.0 cm^2 sec^{-1})
g	gravitational acceleration (980 cm sec^{-2})
T	temperature (℃)
S	salinity (psu)
K_H	horizontal eddy diffusion coefficient (1.0×10^7 cm^2 sec^{-1})
K_V	vertical eddy diffusion coefficient (cm^2 sec^{-1}; values, see Table 2)
H	total depth (cm)
τ	wind stress vector (dyn cm^{-2})
ϕ	total volume transport function
over bar	vertically averaged value

mentioned in sections 4. The summary and discussion will be made in section 5.

2. Model

Figure 1 (b) shows the schematic representation of the model ocean. Coastal and bottom topographies are simplified so that only the main features are modeled. Vertical grid of the numerical model has a relatively thinner thickness in the shallower layer (Fig. 1c), because of large vertical variations in temperature and salinity in the upper layer of the Okhotsk Sea (e. g., YANG and HONJO, 1996).

We adopt a Cartesian coordinate on a β plane with x-axis to the northeast, y-axis to the northwest and z-axis upward. The inclination of x (y) axis from east (north) is 45°. Under the hydrostatic and Boussinesq approximations, the equations of motion are

$$\frac{\partial u}{\partial t}=-\frac{\partial uu}{\partial x}-\frac{\partial uv}{\partial y}-\frac{\partial uw}{\partial z}+fv-\frac{1}{\rho_0}\frac{\partial P}{\partial x}+A_H\left(\frac{\partial^2 u}{\partial x^2}+\frac{\partial^2 u}{\partial y^2}\right)+A_V\frac{\partial^2 u}{\partial z^2} \quad (1)$$

$$\frac{\partial v}{\partial t}=-\frac{\partial uv}{\partial x}-\frac{\partial vv}{\partial y}-\frac{\partial vw}{\partial z}-fu-\frac{1}{\rho_0}\frac{\partial P}{\partial y}+A_H\left(\frac{\partial^2 v}{\partial x^2}+\frac{\partial^2 v}{\partial y^2}\right)+A_V\frac{\partial^2 v}{\partial z^2} \quad (2)$$

$$0=-\frac{1}{\rho}\frac{\partial P}{\partial z}-g \quad (3)$$

where meanings of symbols are tabulated in Table 1.

The continuity equation is

$$\frac{\partial u}{\partial x}+\frac{\partial v}{\partial y}+\frac{\partial w}{\partial z}=0 \quad (4)$$

Conservation equations of temperature and salinity are

$$\frac{\partial T}{\partial t}=-\frac{\partial Tu}{\partial x}-\frac{\partial Tv}{\partial y}-\frac{\partial Tw}{\partial z}+K_H\left(\frac{\partial^2 T}{\partial x^2}+\frac{\partial^2 T}{\partial y^2}\right)+\frac{K_v}{\delta}\frac{\partial^2 T}{\partial z^2} \quad (5)$$

$$\frac{\partial S}{\partial t}=-\frac{\partial Su}{\partial x}-\frac{\partial Sv}{\partial y}-\frac{\partial Sw}{\partial z}+K_H\left(\frac{\partial^2 S}{\partial x^2}+\frac{\partial^2 S}{\partial y^2}\right)+\frac{K_v}{\delta}\frac{\partial^2 S}{\partial z^2} \quad (6)$$

where

$$\delta=\begin{cases}1 & \dfrac{\partial\rho_0}{\partial z}<0\\ 0 & \dfrac{\partial\rho_0}{\partial z}>0\end{cases} \quad (7)$$

In accordance with setting on rigid-lid approximation, it is possible to define a total volume transport function such that,

$$\bar{u}=-\frac{1}{H}\frac{\partial\phi}{\partial y},\quad \bar{v}=\frac{1}{H}\frac{\partial\phi}{\partial x} \quad (8)$$

To eliminate external pressure gradient, barotropic vorticity equation is employed,

$$\frac{\partial Z}{\partial t}=-\beta\bar{u}-\beta\bar{v}-f\left(\frac{\partial\bar{u}}{\partial x}+\frac{\partial\bar{v}}{\partial y}\right)+\frac{1\partial}{H\partial x}\left[\int_{-H}^{0}\left\{-\frac{\partial uv}{\partial x}-\frac{\partial v^2}{\partial y}-\frac{\partial vw}{\partial z}+A_H\left(\frac{\partial^2 v}{\partial x^2}+\frac{\partial^2 v}{\partial y^2}\right)\right\}dz\right]$$

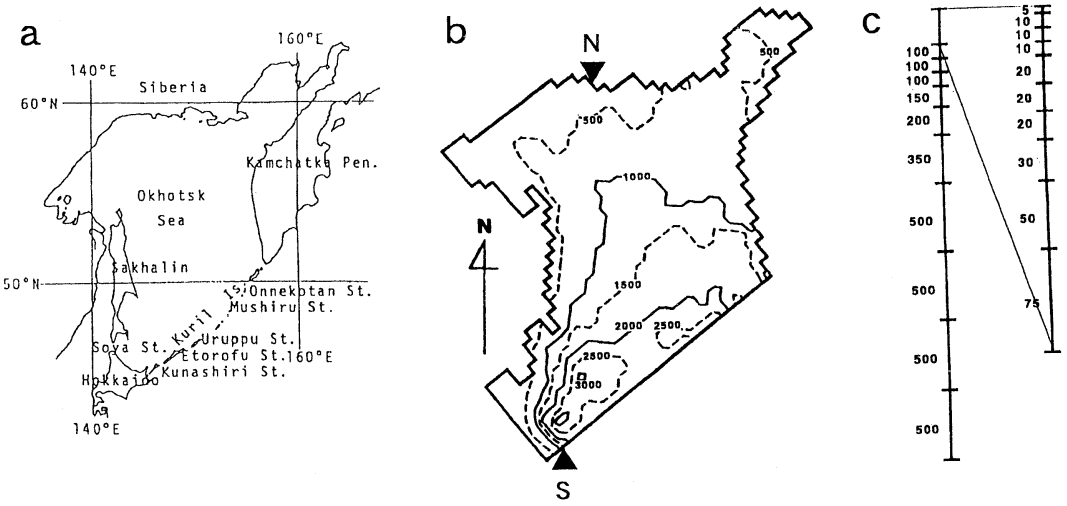

Fig. 1. (a) Map of the Okhotsk Sea. (b) Domain of the model ocean with a simplified bottom topography (isopleth of depth in meter). A pair of black triangles show the location of the meridional cross section of the vertical distributions of calculated temperature, salinity and density fields. (c) Vertical grid distribution showing the thickness (in meter) of each level.

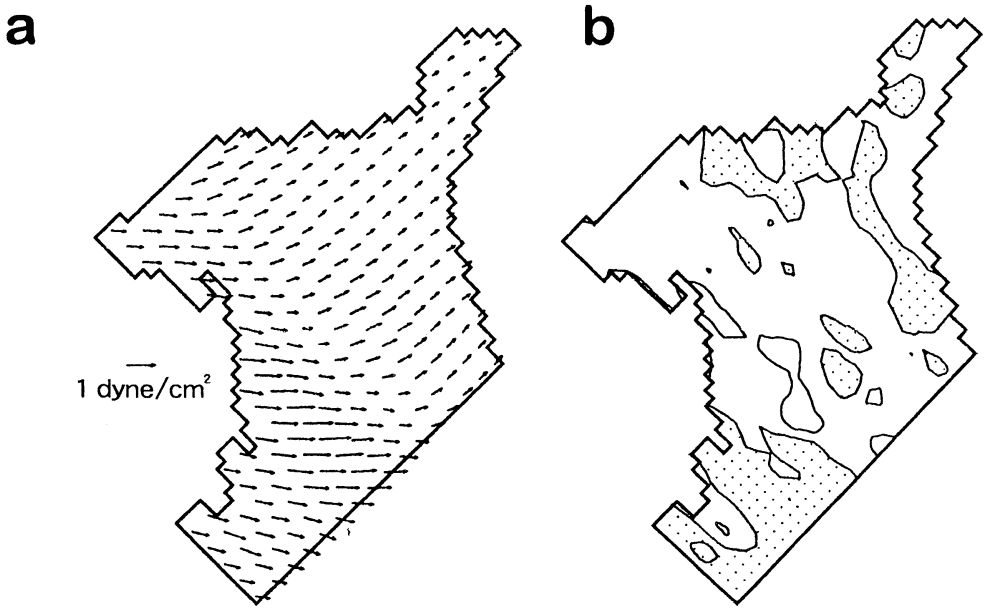

Fig. 2. (a) Annual mean wind stress of the present model. No value below 0.1 dyne cm^{-2} is plotted. (b) Annual mean wind stress curl. Contour interval is 10^{-8} dyne cm^{-3} and negative curl regions are dotted.

Table. 2 Conditions for the experiments.

Model	Vertical eddy diffusivity (K_V; cm^2sec^{-1})	Forcing
Run 1	0.5	wind stress
Run 2	0.1	wind stress
Run 3	2.0	wind stress
Run 4	0.1	wind stress and surface heat flux
Run 5	0.5	wind stress and surface heat flux
Run 6	2.0	wind stress and surface heat flux
Run 7	0.1	wind stress, surface heat and fresh water fluxes
Run 8	2.0	wind stress, surface heat and fresh water fluxes

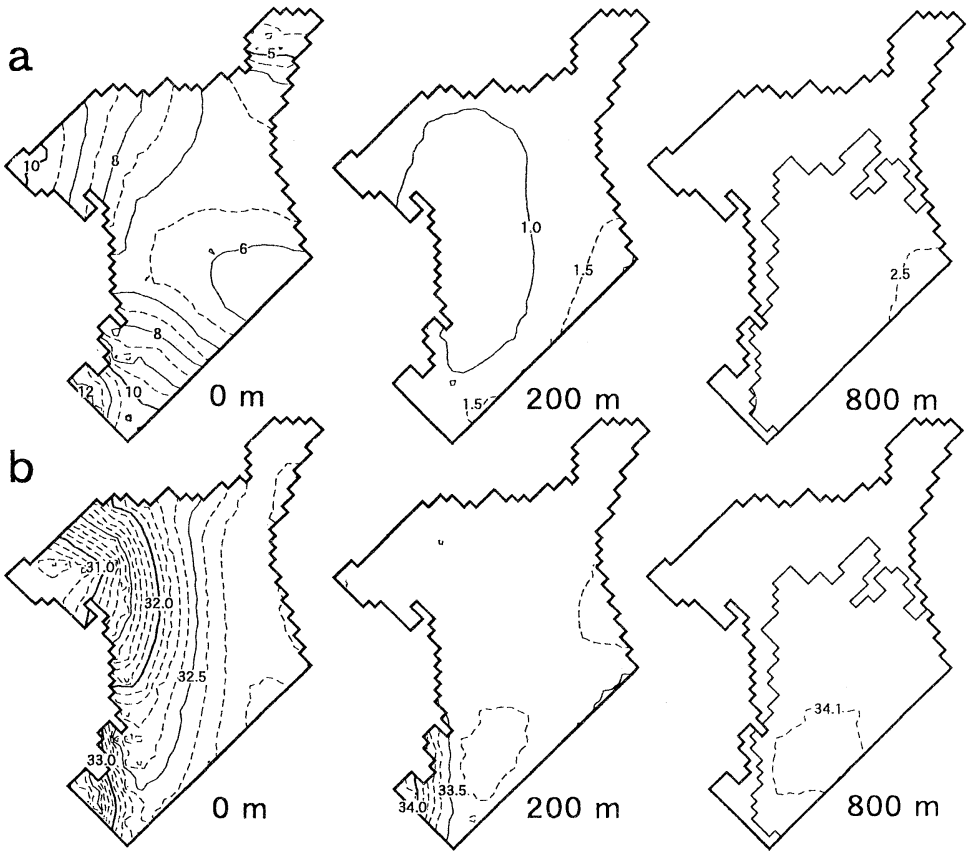

Fig. 3. (a) Initial temperature (in ℃) distributions at the sea surface and the depths of 200 and 800 meters. (b) Same as in (a) but for salinity distributions.

$$-\frac{1}{H}\frac{\partial}{\partial y}\left[\int_{-H}^{0}\left\{-\frac{\partial u^2}{\partial x}-\frac{\partial uv}{\partial y}-\frac{\partial uw}{\partial z}+A_H\left(\frac{\partial^2 u}{\partial x^2}+\frac{\partial^2 u}{\partial y^2}\right)\right\}dz\right]+curl\left(\frac{\tau}{H}\right) \quad (9)$$

where

$$Z=\frac{\partial}{\partial x}\left(\frac{1}{H}\frac{\partial \phi}{\partial x}\right)+\frac{\partial}{\partial y}\left(\frac{1}{H}\frac{\partial \phi}{\partial y}\right) \quad (10)$$

Density of sea water is a function of temperature, salinity and pressure and it is calculated by use of the Joint Panel on Oceanographic Tables and Standards (UNESCO, 1981).

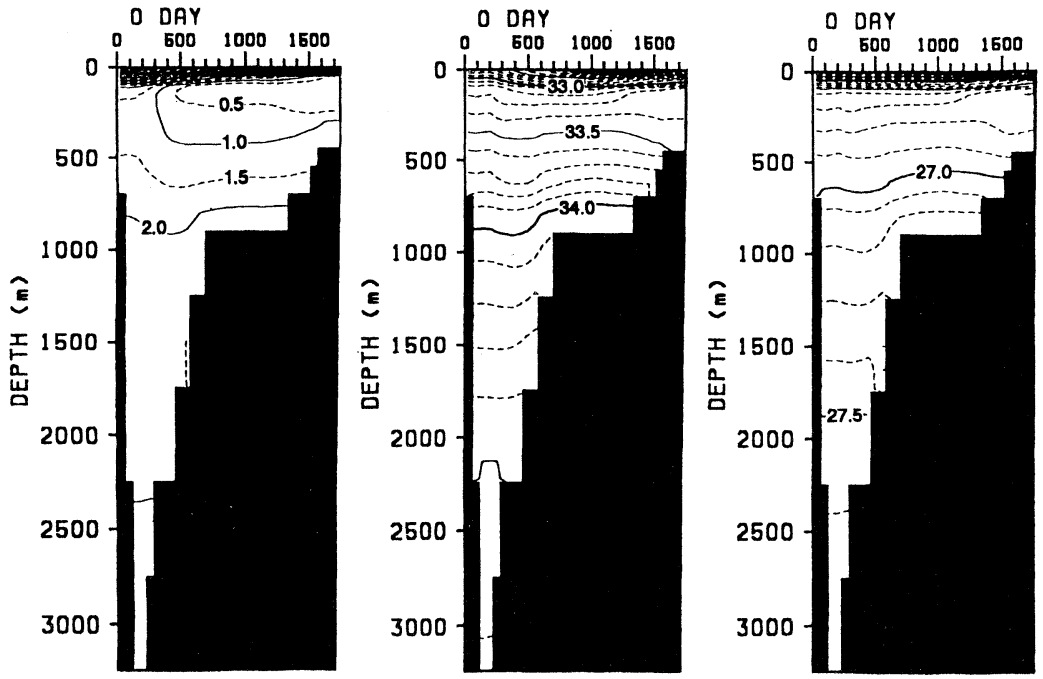

Fig. 4. Vertical distributions of initial temperature (in ℃), salinity (in psu) and σ_θ (kg m^{-3}) along the meridional line shown in Fig. 1 (a). Divisions on top of panels show the distance (in kilometer) from the black triangle labeled S in Fig. 1.

The equations (1)–(10) are solved numerically with the horizontal grid interval of 41.27 km and time interval of 2160 sec. At the upper boundary, following conditions are applied in this study.

$$w = 0$$
$$-\rho_0 A_v\left(\frac{\partial u}{\partial z}, \frac{\partial v}{\partial z}\right) = (\tau_x, \tau_y) \qquad (11)$$
$$-\rho_0 K_v \frac{\partial T}{\partial z} = \frac{Q}{C_p}$$

where τ_x and τ_y are x and y components of the surface wind stress, respectively. C_p is specific heat of sea water and ρ_0 is the density of sea water at surface pressure and standard temperature and salinity. Viscous lateral and bottom boundaries are assumed. No motion is assumed in the initial condition. In order to see the dependence on the intensity of vertical eddy diffusion, three runs with different vertical eddy diffusivity are examined (Table 2) and the circulation is driven by wind stress. In the next, similar three models but for giving the surface heat flux are examined by use of HANEY (1971) formula in which the surface temperature has a tendency to recover mean observed temperature :

$$Q_T = \alpha (T_{obs.} - T_{calc.}) \qquad (12)$$

Here $T_{obs.}$ is the observational sea surface temperature and $T_{calc.}$ is the temperature of the shallowest grid point of the model ocean and α is a constant of 1.0 ly day^{-1}(℃)$^{-1}$. These models are referred to as Runs 4, 5 and 6. Thirdly, we examine two models (Runs 7 and 8) to which surface heat and salinity fluxes are added. Salinity flux is also given by the similar method :

$$Q_s = \alpha (S_{obs.} - S_{calc.}) \qquad (13)$$

Here $S_{obs.}$ is the observational sea surface salinity and $S_{calc.}$ is the salinity at the uppermost grid point of the model ocean.

Maximmum integration time is decided by spatial scale of the Okhotsk Sea and characteristic diffusion time of the thermocline in the Okhotsk Sea. Because zonal spatial scale of the

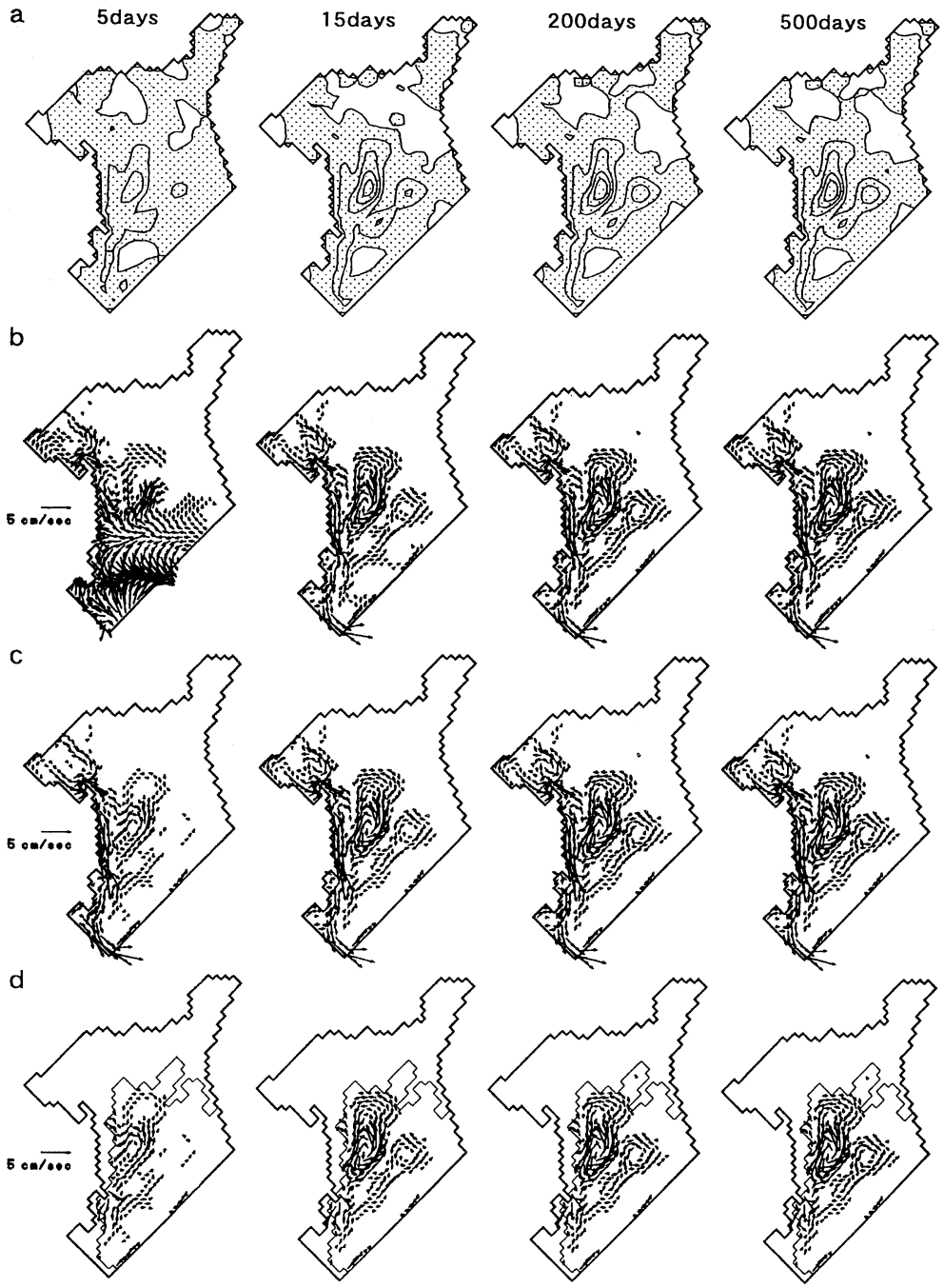

Fig. 5. (a) Horizontal distribution of total volume transport function of Run 1. Contour interval is 1 Sv and regions with the negative stream function are dotted. Horizontal distributions of velocities at (b) 20 m, (c) 200 m and (d) 800m of Run 1. No value below 1 cm sec^{-1} is plotted.

Okhotsk Sea is about 1/5 times as large as that of North Pacific, it takes about 3–5 years to propagate baroclinic Rossby wave in the North Pacific. Therefore, it is expected that baroclinic response in the Okhotsk Sea takes about a year. From a relation between vertical eddy diffusivity ($2.0cm^2/sec$) and thickness of pycnocline in the Okhotsk Sea (100 m), a characteristic diffusion time is estimated about 578 days. Because temperature and salinity distribution in the mixed layer is changed in a year, numerical integration in the present study is carried out by 500 days.

3. Data

Wind stress data used in this study are annual mean observational values, which are linearly interpolated to the grid scale from the $2^\circ \times 5^\circ$ data compiled by KUTSUWADA and SAKURAI (1982). Horizontal distributions of the wind stress and vertical component of curl τ are shown in Fig. 2. Eastward wind stress dominates in the southern region, while northeast wind stress does in the northern region. Since wind stress is relatively weak in spring and summer, the wind stress shown in Fig. 2 mainly represents that in autumn and winter.

The temperature and salinity data compiled by LEVITUS (1994) are used as the initial values of the model (Figs. 3 and 4), which are also linearly interpolated from the $1^\circ \times 1^\circ$ data. Representative characteristics such as the warm saline water off Hokkaido and less saline water in the northwestern part of the Okhotsk Sea by the discharge of Amur River are well shown in upper part of the Okhotsk Sea (Fig. 3). Thermocline, halocline and pycnocline are located in a shallower layer than 200 m (Fig. 4). It is noted that there exists a temperature minimum layer beneath the thermocline.

4. Results

Total volume transport function and horizontal velocities of Run 1 are shown in Fig. 5. A cyclonic circulation is formed east off Sakhalin and relatively strong flow is seen along the coastal lines of Sakhalin and Hokkaido. Total volume transport function has a tendency to run along isobath of the bottom topography. It is also shown that velocity field has a vertically coherent structure, which suggests the barotropic structure of the velocity field. After 200 days, few variations, while detected and results in Fig. 5 are almost stationary state. Barotropic flow is dominant in the velocity field of Run 1 and baroclinic flow is very weak. For this reason, it is suggested that thickness of thermocline is thin and $\partial \rho / \partial z$ is relatively small under the thermocline. Distributions of the total volume transport functions of Runs 2 and 3 (Fig. 6) are almost similar to those of Run 1 (Fig. 5). These results show that the flow pattern driven by wind stress is not altered by the intensity of vertical eddy diffusion.

Temperature and salinity distributions of Run 1 at sea surface and the depth of 200 m are shown in Fig. 7. At sea surface, temperature and salinity gradients are weaker than initial temperature and salinity gradients, respectively. Temperature and salinity at the depth of 200 m are lower than those at initial state (Fig. 4), which is mainly due to vertical diffusion of minimum temperature layer. Temperature distributions of Run 5 are higher than those of Run 1 (Fig. 7c). At the depth of 200 m, it is seen that temperature gradient of Run 5 is stronger than that of Run 1. Vertical distributions of temperature salinity and σ_θ of Runs 4 6 are shown in Fig. 8. Temperature field of Run 5 has a tendency to be vertically homogeneous, which is different from observational temperature field shown in Fig. 4. Because σ_θ field is changed by the increase in temperature, isopycnal slopes are increased at a depths 300 m–2000 m. Although σ_θ gradient is commonly formed in three runs shown in Fig. 8, horizontal velocity distributions of these runs are vertically coherent (Fig. 9). This is similar to those of previous three runs shown in Fig. 5.

Difference of the horizontal velocity of Run 4 from that of Run 6 is shown in Fig. 10. Near the coastal line of the Sakhalin Island, directions of the differences are same as the velocity of Runs 4 and 6. On the contrary, the differences near the coastal line of the Hokkaido are in the opposite direction of the velocity of Runs 4 and 6. Experiments are also examined in the case that heat and salinity fluxes are given at the sea surface (Runs 7 and 8). In these cases, clear difference from others is not seen in the velocity

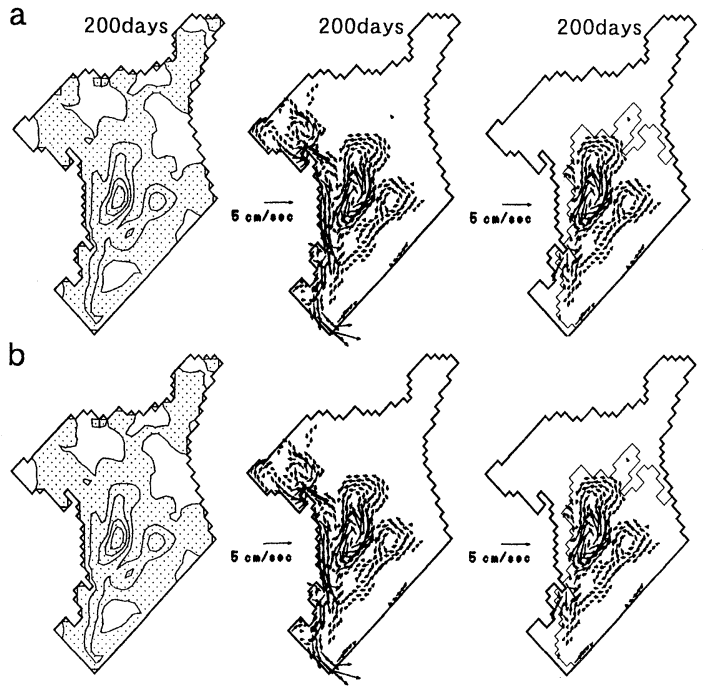

Fig. 6. Horizontal distributions of stream function (left), velocity at 200 m (middle) and that at 800m (right) of (a) Run 2 and (b) Run 3. Contour interval is 1 Sv and regions with the negative stream function are dotted. No value below 1 cm sec^{-1} is plotted.

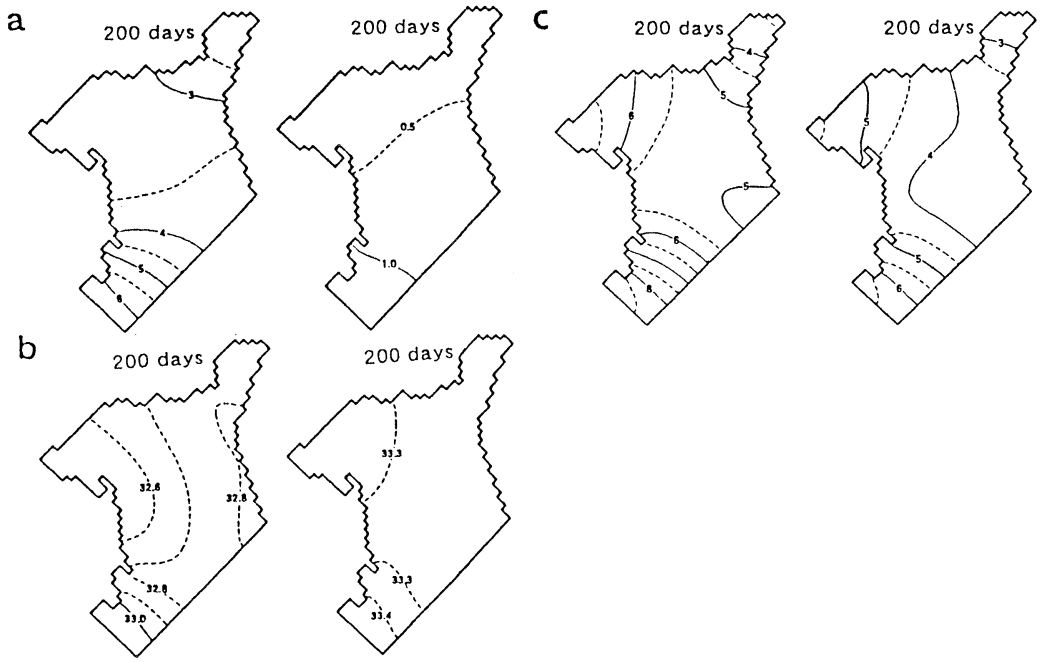

Fig. 7. (a) Temperature distributions at sea surface (left) and depth of 200 m (right). of Run 1 (b) Same as in (a) but for salinity, (c) Same as in (∂) but for temperature of Run 5.

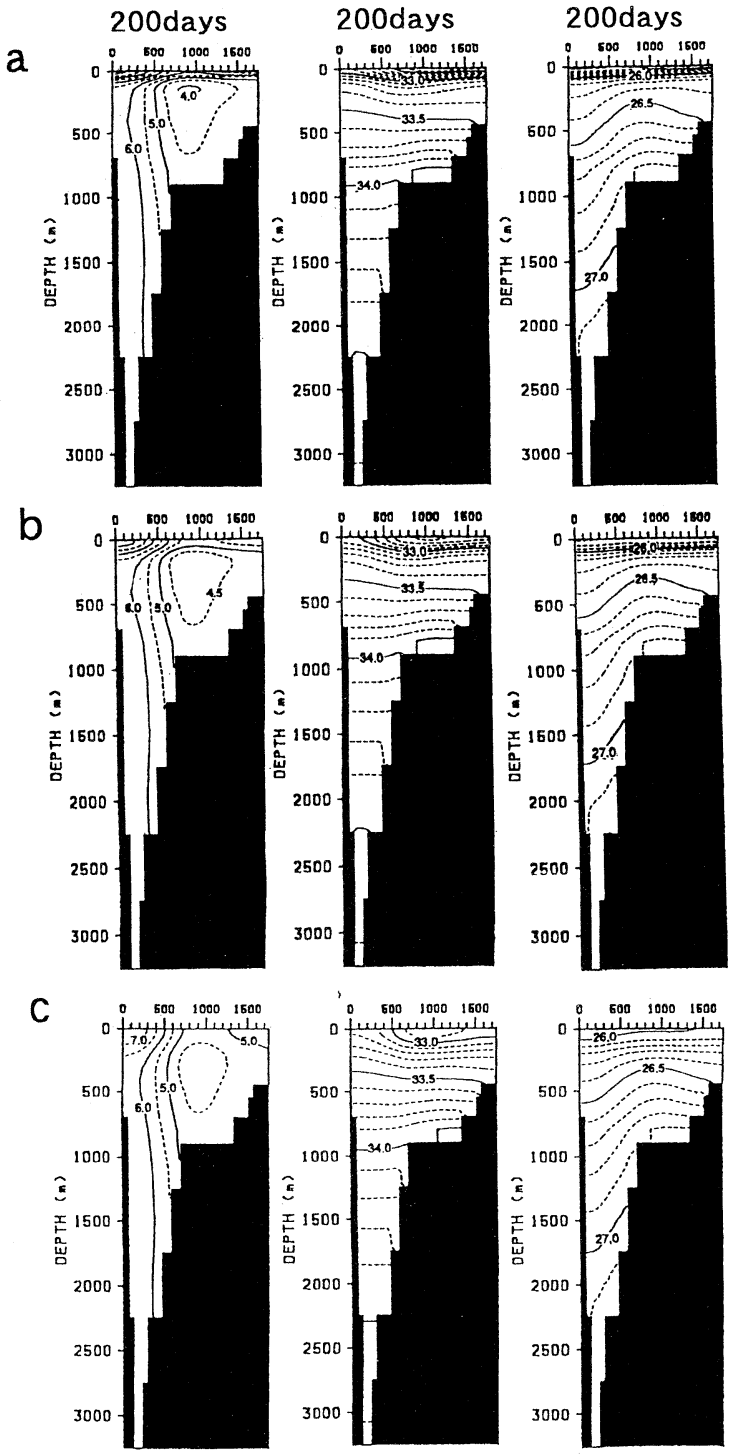

Fig. 8. Vertical distribution of temperature (left), salinity (middle) and σ_θ (right). Contour intervals and divisions on top of panels are the same as in Fig. 4. (b) Run 5. (c) (a) Run 4, Run 6.

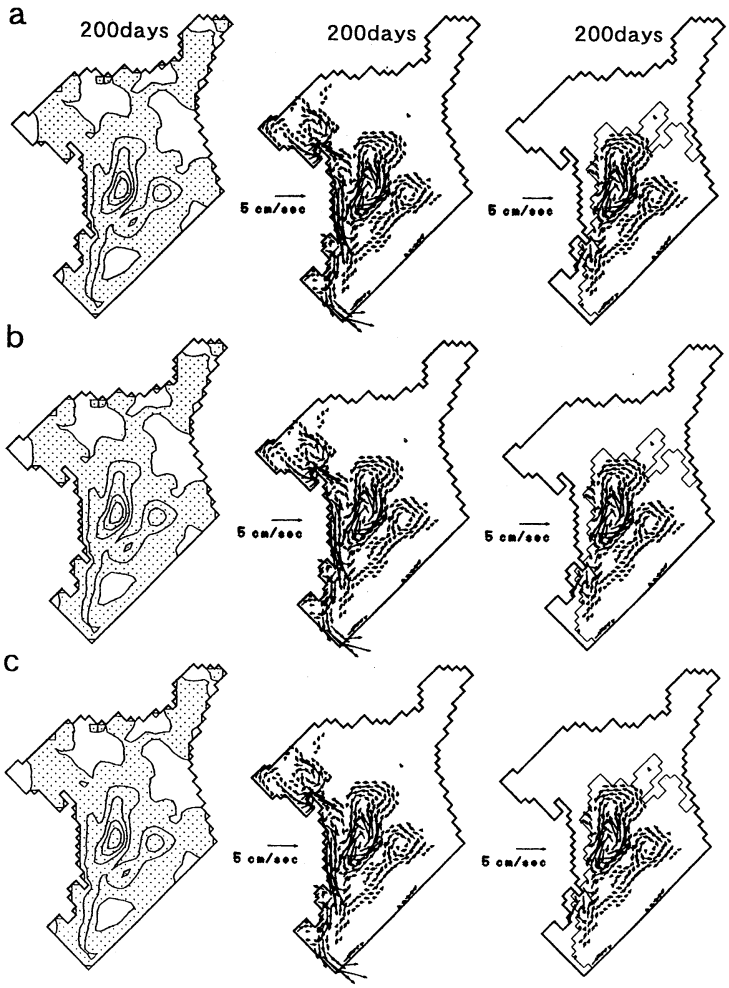

Fig. 9. Same as in Fig. 6 (a) but for (a) Run 4, (b) Run 5 and (c) Run 6.

field. The velocity difference which is larger than 10^{-3} cm sec^{-1} is detected east of Sakhalin and near the coastal line of the Hokkaido (Fig. 11). However, both differences are very small and the order of 10^{-3} cm sec^{-1}. These results indicate that effects of surface heat and salinity fluxes are weak for the general circulation in the Okhotsk Sea. It shows that the barotropic flow pattern is dominant in the Okhotsk Sea, which is not influenced by the intensity of vertical eddy diffusivity.

5. Summary and discussion

Oceanic circulation in the Okhotsk Sea is examined numerically with special reference to its dependence of the intensity of vertical eddy diffusivity.

It is commonly resulted that total volume transport function has a tendency to run along isobaths of the bottom topography and velocity field has a vertically coherent structure. These results imply that the barotropic flow structure dominates in the velocity field of the Okhotsk Sea, which is not influenced by the intensity of vertical eddy diffusivity. It is also resulted that the wind driven circulation dominates in comparison with the thermohaline driven circulation.

Firstly, weakness of vertical density gradient is assigned as a reason for the above results.

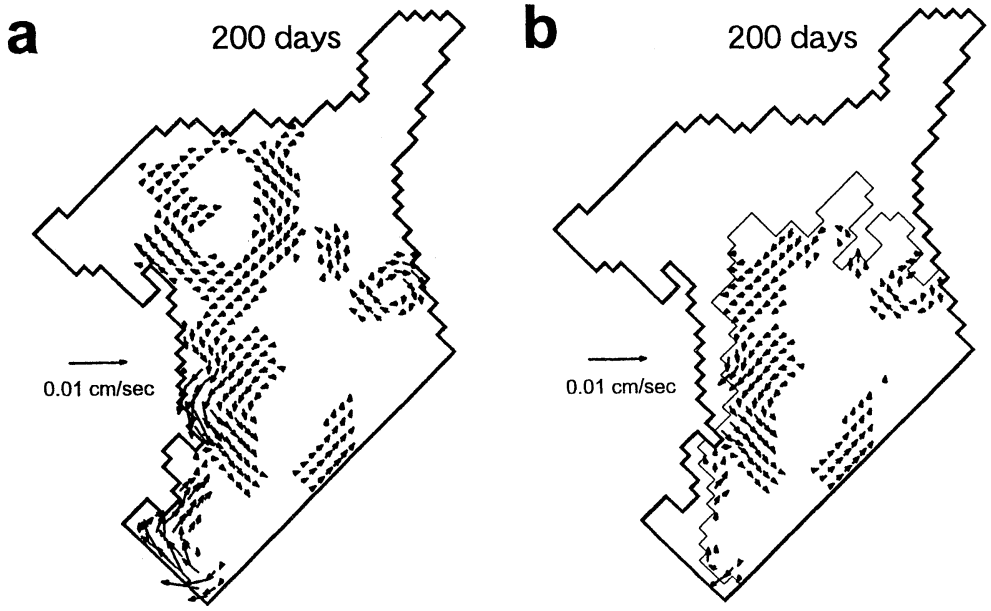

Fig. 10. Horizontal distributions of the difference of velocity field of Run 4 from that of Run 6 (a) at 200 m and (b) 800m. No value below 10^{-2} cm sec^{-1} is plotted.

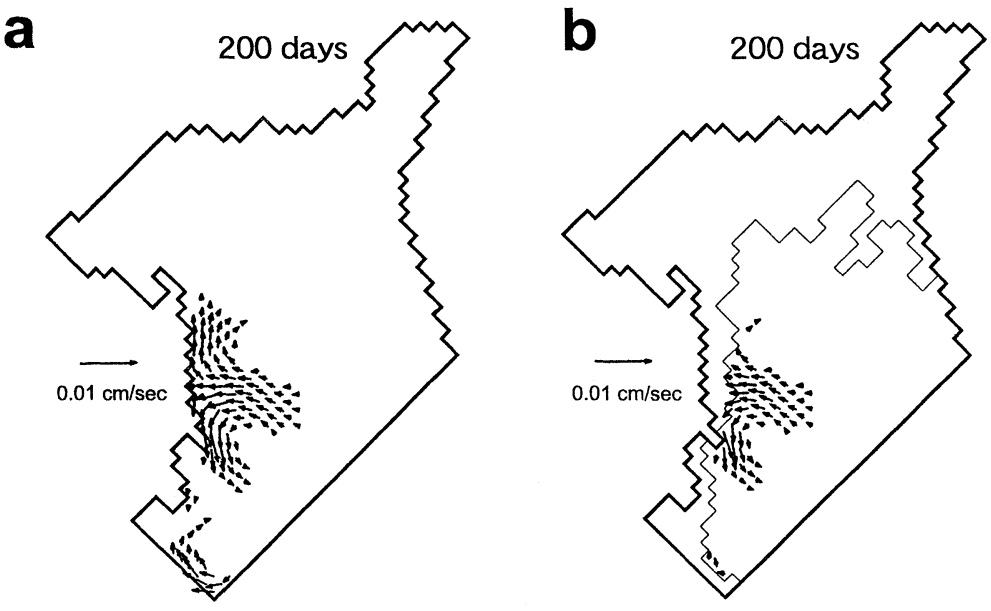

Fig. 11. Same as in Fig. 10 but for the difference of Run 7 from Run 8.

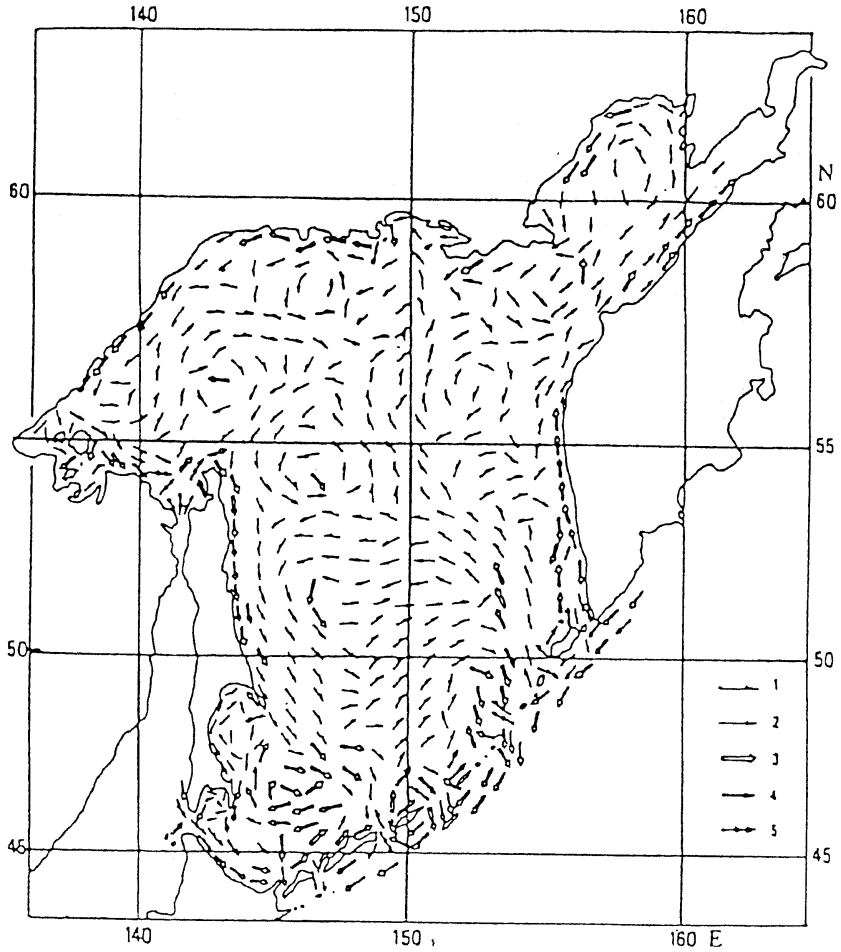

Fig. 12. Surface current velocity in August estimated by the geostrophic balance referred to 2000 db (M OROSHKIN, 1964). Five kinds of arrows noted by 1, 2, 3, 4 and 5 show the current velocity $<5\text{cm s}^{-1}$, 5cm s^{-1}–10cm s^{-1}, 10cm s^{-1}–20cm s^{-1}, 20cm s^{-1}–30cm s^{-1} and $30\text{cm s}^{-1}<$, respectively.

Generally, characteristic velocity of thermohaline driven circulation (U_t) is estimated by the following equation (BRYAN, 1987) :

$$U_t = \left[\left(\frac{g^*}{f}\right)^2 \left(\frac{K_v}{L}\right)\right]^{\frac{1}{3}}$$

where g^* and L are reduced gravity and horizontal scale of thermohaline velocity distribution, respectively. From above equation, magnitude of thermohaline driven circulation depends on strength of density stratification in addition to vertical eddy diffusivity. It is thus suggested that weakness of the thermohaline driven is caused by vertical density structure of the Okhotsk sea. Secondly, horizontal scale of the Okhotsk sea is smaller than that of the Pacific ocean and/or the Atlantic ocean in which the velocity field depend on vertical eddy diffusivity. Strength of thermohaline driven circulation is generally decided by magnitude of available potential energy. Because spatial scale of the Okhotsk Sea is much smaller than that in the North Pacific and/or North Atlantic, meridional thermal difference is small in the Okhotsk Sea. There is a possibility that independence of vertical eddy diffusivity is caused by the difference between their spatial scales.

On the other hand, cyclonic eddy east off Sakhalin seen in Runs 1–6 is qualitatively similar to that of the observational geostrophic map (Fig. 12), so it will be formed by the wind stress. Oceanic circulation driven by in-and outflow and that driven by seasonal wind stress have not been included in the present study. These points should be examined in the next stage of this study.

Acknowledgments :

The numerical calculations were carried out on a FACOM M-1800 of Nagoya University and on a FACOM M-760 of Mie University. This study was supported by Global Ocean Observational System (GOOS). We would like to thank Mr. N. UDA of Information Processing Center of Mie University for his help in calculation. We also wish to thank the anonymous reviewer for his many helpful comments.

References

BRYAN, F. (1987) : Parameter sensitivity of primitive equation ocean general circulation models. J. Phys. Oceanogr., **17**, 970–985.

HANEY, R. L. (1971) : Surface thermal boundary condition for ocean circulation model. J. Phys. Oceanogr., **1**, 241–248.

KAJIURA, K. (1949) : On the hydrography of the Okhotsk Sea in summer. J. Oceanogr. Soc. Japan, **5**, 19–26 (in Japanese).

KITANI, K. (1973) : An oceanographic study of the Okhotsk Sea. Bull. Far Seas Res. Lab., **9**, 45–77.

KITANI, K. and K. SHIMAZAKI (1971) : On the hydrography of the northern part of the Okhotsk Sea in summer. Bull. Fac. Fish. Hokkaido Univ., **12**, 231–242 (in Japanese).

KUTSUWADA, K. and K. SAKURAI (1982) : Climatological maps of wind stress field over the North Pacific. Oceanogr. Mag., **32**, 25–46.

KURASHINA, S. (1986) : Water exchange in the Okhotsk Sea. Marine Sci., **18**, 123–127 (in Japanese).

LEVITUS, S. (1994) : World Ocean Atlas 1994.

MOROSHKIN, K. B. (1964) : A new surface current map in the Okhotsk Sea. Okeanologia, **4**, 614–643 (in Russian).

SEKINE, Y. (1990) : A barotropic numerical model for the wind-driven circulation in the Okhotsk Sea. Bull. Fac. Bioresouces, Mie Univ., **3**, 25–39.

UNESCO (1981) : Thenth report of the joint panel on oceanographic tables and standards, UNESCO Technical Papers in Marine Science, 36, 192pp.

WAKATSUCHI, M. and S. MARTIN (1991) : Water circulation of the Kuril Basin of the Okhotsk Sea and its relation to eddy formation. J. Oceanogr. Soc. Japan. **47**, 152–168.

YANG, J. and S. HONJO (1996) : Modeling the near-freezing dichothermal layer in the Sea of Okhotsk and its interannual variations. J. Geophys. Res. **101**, 16421–16433.

ZHANG, S., C. A. LIN and R. GREATBATCH (1992) : A thermocline model for ocean-climate studies. J. Mar. Res., **50**, 99–124.

Received December 4, 1997
Accepted March 15. 1999